Response of Ionospheric WN4 to Atmospheric ITCZ

Cheng, C. C[1], J. Y. Liu[1,2,3]

[1] Graduate Institute of Space Science and Engineering, National Central University, TAIWAN

[2] Center for Astronautical Physics and Engineering, National Central University, TAIWAN

[3] Center for Space and Remote Sensing Research, National Central University, TAIWAN

Abstract

The ion density, ion temperature, and ion velocity probed by ROCSAT-1 and DEMETER (Detection of Electro Magnetic Emissions Transmitted from Earthquake Regions) are used to examine the daytime wavenumber-4 (WN4 or four-peak) feature within magnetic latitude ±15˚ during the high solar activity period of 1999-2004 (F10.7>104.9 sfu) and low solar activity period of 2005-2011 (F10.7<104.9 sfu). The quasi-neutrality of the ion and electron density and the Coulomb collision effect of the ion (electron) density and ion (electron) temperature confirm that DEMETER and ROCSAT-1 data are reliable. During the high solar activity period, the correlation coefficient of WN4 variations between the ion density of δN_i and upward ion velocity of δV_z is a positive value and proportional to the solar activity. However, during the low solar activity period, the correlation coefficient between δN_i and δV_z is about zero and no clear relationship can be found. In contrast, δN_i and WN4 variations in the northward ion velocity of δV_x generally yield anti-correlation during the low solar activity period, and however no clear relationship can be found during high solar activity period. Based on the dynamo theory, the eastward electric field derived by δV_z ranges from -0.11 to +0.11 mV/m in the high solar activity. This confirms that WN4 becomes prominent in daytime during high solar activity periods

1. Introduction

Wavenumber-four (WN4 or four-peak) structures in the nighttime OI 135.6-nm emission along the geomagnetic equator were observed by IMAGE and TIMED satellites [*Sagawa et al.*, 2005; *Henderson et al.*, 2005]. *Sagawa et al.* [2005] examined the global characteristics of the nighttime equatorial ionization anomaly (EIA) by constructing a constant local time (LT) map that shows the development of the EIA with a significant longitudinal structure, in which peaks and troughs of the OI 135.6-nm emission intensity along the crest latitude have about 90˚ longitudinal separation in the longitude range from 0˚ to 250˚. *Immel et al.* [2006] also found that four longitudinal peaks in 135.6-nm brightness observed on both sides of the geomagnetic equator are in near coincidence with four maxima of tidal temperature at 115 km altitude, and proposed that the diurnal or semidiurnal eastward wave number three (DE3 or SE3) nonmigrating tides excited from the lower atmosphere propagates upward to the lower ionosphere and subsequently affects the E-region dynamo electric field, which results in the WN4 feature. *Hartman and Heelis* [2007] and *Kil et al.* [2007] observed WN4 signatures in vertical ion drift velocity near the magnetic equator by means of in situ DMSP and ROCSAT-1 observations. *Kil et al.* [2008] and *Fejer et al.* [2008] reported that during the daytime equinox and June solstice, topside ionosphere WN4 peaks in vertical ion drift velocity appear collocated with longitudinal maximums in ion density.

Monthly and solar cycle variations of WN4 features as well as the correlation between the ion and electron density/temperature; ion/electron density and temperature; ion density and ion velocity; and ion density and eastward electric fields under different solar flux conditions is revealed in this study.

2. Data Analysis

Republic of China Satellite 1 (ROCSAT-1) had a circular orbit at an average altitude of 600 km with an inclination of 35˚ and provided data from January 1999 to June 2004. Its low-inclination orbit enabled ROCSAT-1 to sample the ionosphere at the magnetic equator during all local times approximately every 25 days. Detection of Eletro-Magnetic Emissions Transmitted from Earthquake Regions (DEMETER) was launched on 29 June 2004 in the circular sun-synchronize orbit with inclination of 98˚ and 660~730 km altitude. Local time of the descending and ascending node is 1030 LT and 2230 LT. DEMETER provided data from July 2004 to March 2011 covering within ±65˚ geomagnetic latitude and its revisiting time is about 16 days. Monthly data during 0900-1100LT are selected to develop the constant LT map to examine daytime WN4 features. To remove highly fluctuated and unwanted noises obtaining smoothed LT maps, a window of 20˚ latitude and 20˚ longitude, acting as a low-pass filter, by sliding 2˚ in latitude and 10˚ in longitude is applied on ROCSAT-1 data, while another one using window of 20˚ latitude by 30˚ longitude with the same sliding is applied on DEMETER data. However, the peak over around 0˚ is very weak. To further recognize the WN4 feature, large scale variations are removed by calculating the deviation data δA

$$\delta A = \mathrm{smooth}(A) - \mathrm{median}(A) \quad (1)$$

where smooth(A) is the smoothed LT map, and median(A) is calculated by the 90˚ (i.e. ±45˚) longitudinal running median. *Kil et al.* [2007] and *Fejer et al.* [2008] proposed that the accuracy of the velocity measurement from the ion drift meter depends on the proportion of oxygen ions (O^+) and light ions. The cross-track ion velocity can be determined accurately (error <10%) when O^+ density is greater than 85%, meaning less light ions such as hydrogen ions (H^+), and this condition is satisfied in most cases at 600 km. Therefore, plasma data that measured by the ion drift meter with the percentage of H+ above 15% have been removed in this study.

3. WN4 Feature Observation

Responses of daytime plasma quantities of the electron/ion density (N_e and N_i), electron/ion temperature (T_e and T_i), and ion velocity to WN4 probed by ROCSAT-1 and DEMETER in various months, years and solar activities during the geomagnetic quiet (Kp≤3) are examined. Meanwhile, based on the dynamo theory [*Kelly*, 2009], ionospheric eastward electric fields E_{yz} and E_{yx} can be derived by the upward ion velocity V_z and northward ion velocity V_x, respectively

Figure 1 reveals clear WN4 features in δN_i and δT_i over the center of Pacific Ocean (PO), the west side of Southern American (SA), the center of Atlantic Ocean (AO), and the Southern India (SI) in all seasons especially from July to November. In 1999-2004, prominent features in δV_z and δE_{yz} exist in March and September-November. WN3 features in δE_{yx} over PO, AO, and SI in January-March and September-November. In 2004-2010, δN_i and δT_i also exhibit WN4 features in all seasons, while there is a depletion in δN_i and an enhancement in δT_i over AO in June. Notice that the WN4 signature in δN_i, δT_i, δV_z, and δE_{yz} over SA shifts toward east in January-June and toward west in July-December 1999-2010.

Figure 2 presents the correlations between δN_i and δV_z, δN_i and δV_x, δN_i and δE_{yz}, as well as δN_i and δE_{yx} probed by ROCSAT-1 during the high solar activity and by DEMETER during the low solar activity, respectively. Based on the linear regression, both correlation coefficients and slopes between the above two parameters are calculated. The correlation coefficients R = 0.60 (0.57, 0.63) between δV_z and δN_i confirms a positive correlation during the high solar activity, while R = 0.05 (-0.09, -0.02) indicates no clear correlation during the low solar activity. Owing to the correlation between δV_z and δN_i being positive, the eastward electric field associated with WN4 can be derived by δV_z and the earth's magnetic field (Eq. (2)), which ranges from -0.11 to +0.11 mV/m during the high solar activity. On the other hand, it is interesting to find R = 0.50 (0.47, 0.53) between δN_i and δE_{yx} but no clear correlation with R = 0.08 (0.04, 0.12) between δN_i and δV_x. Response of the correlation coefficient between δV_z (δE_{yz}) and δN_i as well as δV_x (δE_{yx}) and δN_i to the solar activity in various months of years are further examined. Figure 3 reveals that coefficients between δV_z (δE_{yz}) and δN_i as well as δE_{yx} and δN_i, are positive in various months during the high solar activity years. In contrast, the coefficients are fluctuated around zero during the low solar activity years. Figure 4 illustrates response of coefficients to the solar activity. To avoid the seasonal variation, the 12-month running mean, which has been used to derive the well-known R_{12}, of coefficients and F10.7. The positive correlation coefficients of δV_z-δN_i, δE_{yz}-δN_i, and δE_{yx}-δN_i are both proportional to the solar radiation flux when F10.7>107.6 sfu. It is interesting to find that the saturation effect between coefficients and F10.7 appears at F10.7=114.2 sfu. In contrast, coefficients are mainly negative when F10.7<107.6 sfu.

4. Discussion and Conclusion

Satellite measurements of TOPEX TEC [*Scherliess et al.*, 2008], ROCSAT-1 ion density/velocity [*Kil et al.*, 2008; *Fejer et al.*, 2008], DEMETER and Hinatori ion/electron density/temperature [*Kakinami et al.*, 2011], DMSP ion density [*Hawkin et al.*, 2017], and FORMOSAT-3/COSMIC electron density, *Nm*F2, and *hm*F2 [*Onohara et al.*, 2018] yield prominent WN4 features in the March and September equinoxes, while Figure 1 reveals most pronounced WN4 features of δN_i and δT_i appear in March and September 1999-2011, and those of δV_i and δE_{yz} appear in March, June, and September 1999-2004. *Kil et al.* [2008] and *Fejer et al.* [2008] examined diurnal variations of the upward drift, V_z, in various months and found that the daytime ROCSAT-1 upward drifts V_z have strong WN4 signatures in the morning during equinox and June solstice during the high solar activity, which generally agree with patterns of δV_z in Figure 1. Note that response of the WN4 feature in δE_{yz} to solar activities has not yet been discussed. Figure 2 shows the positive correlation between δE_{yz} (δE_{yx}) and δN_i around the magnetic equator, ±15˚, observed by ROCSAT-1, which indicates that eastward electric fields are essential to WN4 features in δN_i during the high solar activity. The value of δE_{yz} derived from Eq. (2) is in agreement with that derived from the empirical vertical drifts model constructed by *Fejer et al.* [2008]

In conclusion, the positive correlation coefficient between δN_i and δV_z (δE_{yz}) as well as δN_i and δE_{yx} exhibits during the high solar activity and is proportional to the solar radiation. The eastward electric field derived by δV_z within geomagnetic latitude ±15˚ ranges from -0.11 to +0.11 mV/m during the high solar activity. On the contrary, no pronounced association between δN_i and δV_z (δE_{yz}) as well as δN_i and δE_{yx} can be observed during the low solar activity.

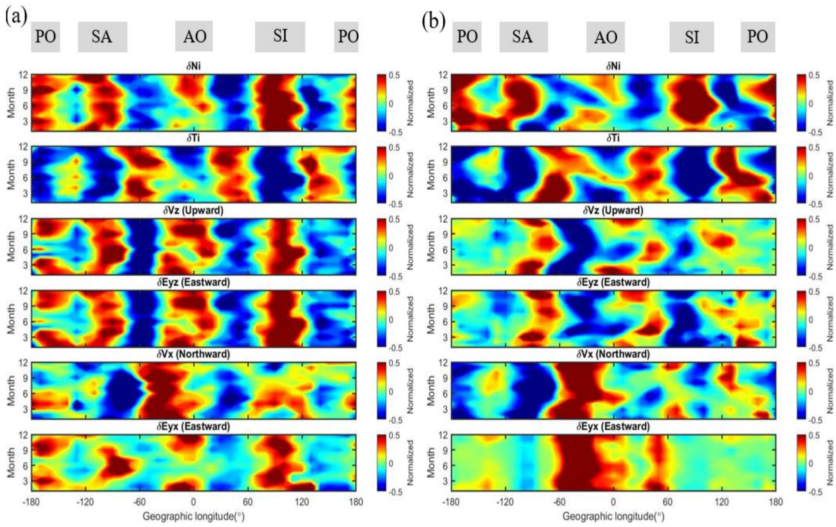

Figure 1 Monthly variations of deviation plasma quantities within geomagnetic latitude ±15˚ in 1999-2010. (a) ROCSAT-1 at 0900-1100LT in 1999-2004, and (b) DEMETER at 1030LT in 2004-2010.

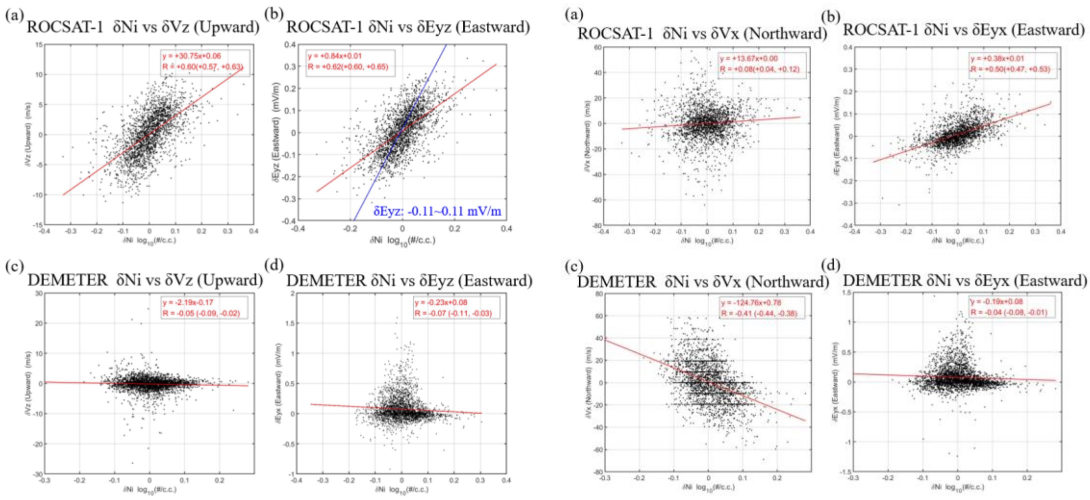

Figure 2 The scatterplot of δN_i versus δV_z and δN_i versus δE_{yz} observed by ROCSAT-1 in July 1999-May 2004 (top) and DEMETER in July 2004-March 2011 (bottom). The lower and upper bound for a 95% confidence interval for each R are presented in the parentheses.

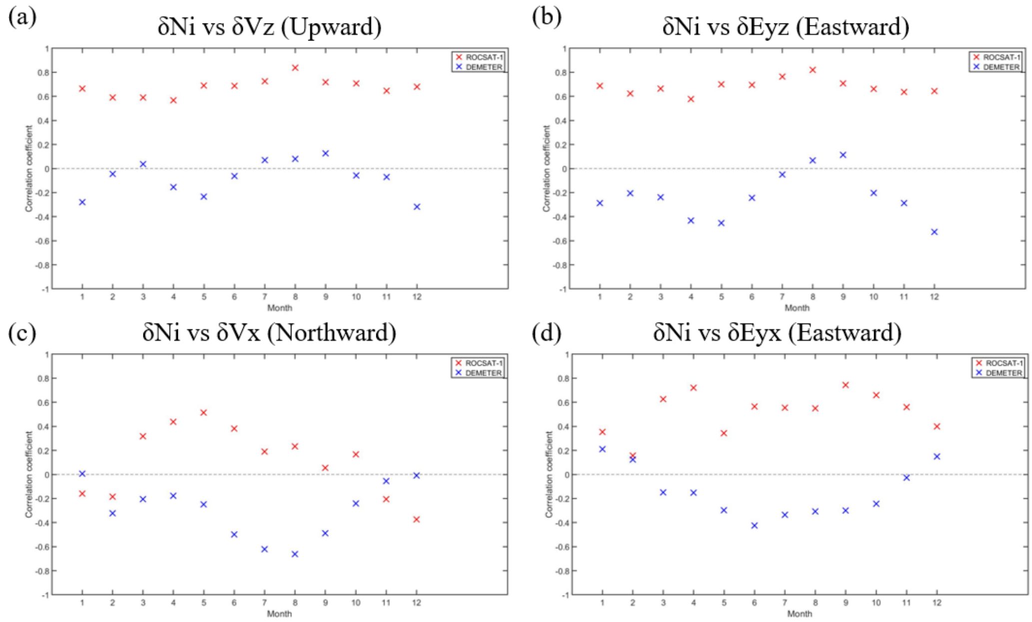

Figure 3 The median of correlation coefficients of linear regression between δV_z (δE_{yz}) and δN_i as well as δV_x (δE_{yx}) and δN_i in each month during the ROCSAT-1 and DEMETER mission period.

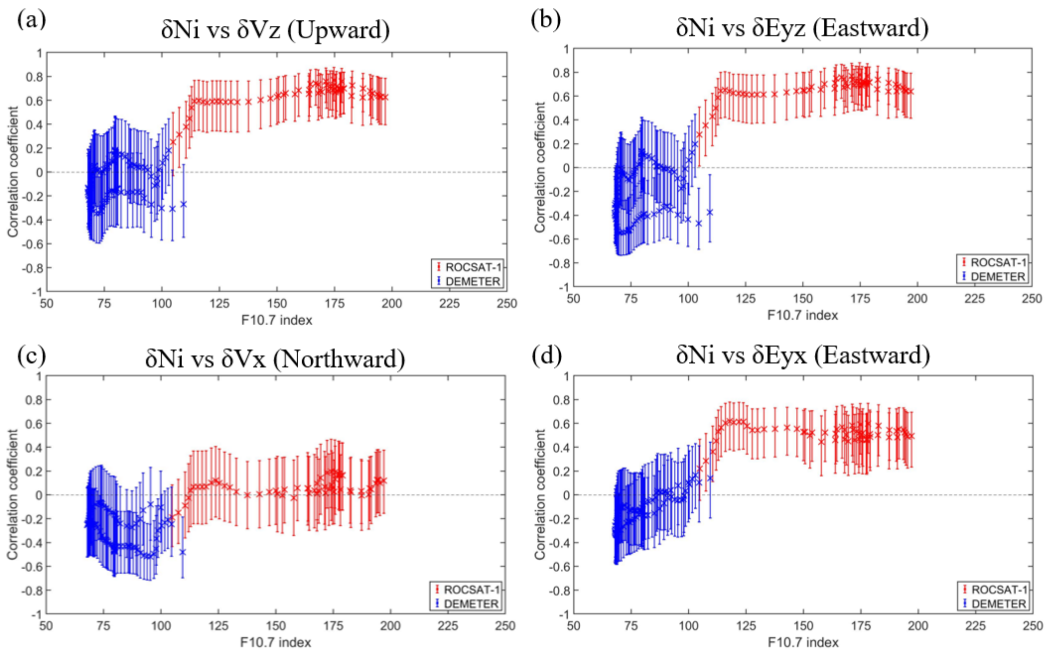

Figure 4 The scatterplot of F10.7 index versus correlation coefficients. The errorbars are lower and upper bounds for a 95% confidence interval for each coefficient. The black lines in the upper and bottom panel are the linear regression line of ROCSAT-1 data.

Reference

Fejer B. G., J. W. Jensen, and S. Y. Su (2008), Quiet time equatorial F region vertical plasma drift model derived from ROCSAT-1 observations, *J. Geophys. Res.*, VOL. 113, A05304, doi:10.1029/2007JA012801

Hartman W. A. and Heelis R. A. (2007), Longitudinal variations in the equatorial vertical drift in the topside ionosphere, *J. Geophys. Res. Space Physics*, VOL. 112, A03305, doi:10.1029/2006JA011773

Hawkins, J. M., and P. C. Anderson (2017), WN4 variability in DMSP ion densities across season, solar cycle, and local time, *J. Geophys. Res. Space Physics*, 122, 8755–8769, doi:10.1002/2017JA024065.

Immel T. J., E. Sagawa, S. L. England, S. B. Henderson, M. E. Hagan, S. B. Mende, H. U. Frey, C. M. Swenson, and L. J. Paxton (2006), Control of equatorial ionospheric morphology by atmospheric tides, *Geophys. Res. Lett.,* vol. 33, L15108, doi:10.1029/2006GL026161

Kakinami Y., C. H. Lin, J. Y. Liu, M. Kamogawa, S. Watanabe, and M. Parrot (2011), Daytime longitudinal structures of electron density and temperature in the topside ionosphere observed by the Hinotori and DEMETER satellites, *J. Geophys. Res. Space Physics*, VOL. 116, A05316, doi:10.1029/2010JA015632

Kil H., S.-J. Oh, M. C. Kelley, L. J. Paxton, S. L. England, E. Talaat, K.-W. Min, and S.-Y. Su (2007), Longitudinal structure of the vertical E x B drift and ion density seen from ROCSAT-1, *Geophys. Res. Lett.,* VOL. 34, L14110, doi:10.1029/2007GL030018

Kil H., E. R. Talaat, S.-J. Oh, L. J. Paxton, S. L. England, and S.-Y. Su, Wave structures of the plasma density and vertical E × B drift in low-latitude F region (2008), *J. Geophys. Res.,* vol. 113, A09312, doi:10.1029/2008JA013106

Onohara A. N., I. S. Batista, and P. P. Batista, Wavenumber-4 structures observed in the low-latitude ionosphere during low and high solar activity periods using FORMOSAT/COSMIC observations (2018), *Ann. Geophys., 36, 459–471*, https://doi.org/10.5194/angeo-36-459-2018

Sagawa E., T. J. Immel, H. U. Frey, and S. B. Mende, Longitudinal structure of the equatorial anomaly in the nighttime ionosphere observed by IMAGE/FUV (2005), *J. Geophys. Res.,* vol. 110, A11302, doi:10.1029/2004JA010848

Scherliess L., D. C. Thompson, and R. W. Schunk (2008), Longitudinal variability of low-latitude total electron content: Tidal influences, *J. Geophys. Res.* VOL. 113, A01311, doi:10.1029/2007JA012480